

Cross Track Error and Proportional Turning Rate Guidance of Marine Vehicles

Fotis A. Papoulias*

The problem of turning rate guidance and control of marine vehicles is considered. Feedback with feedforward rudder control is used to deliver a specified turning rate for the vehicle, while a guidance law is employed to create the necessary sequence of turning rate commands which would allow convergence to a desired geographical path. Two different guidance schemes are presented and analyzed, namely, cross track error and proportional turning rate guidance. Stability conditions are computed explicitly, while nonlinear analysis techniques illustrate the significance of design parameters on the final system response that cannot be inferred from linearized stability results.

Introduction

SMALL UNMANNED marine vehicles suitable for use in both naval and commercial operations have unique mission requirements and dynamic response characteristics. In particular, they are required to be highly maneuverable and very responsive as they operate in obstacle-avoidance and object-recognition scenarios. The need, therefore, arises to maintain accurate path-keeping in confined spaces and shallow waters under the influence of steady- and time-varying external forces. The primary vehicle guidance system is based on heading or turning rate commands that are generated based on a specified geographical sequence of desired way points. Speed commands can be generated by incorporating temporal attributes to the way points. These guidance commands are then passed to the vehicle controller which attempts to deliver the commanded heading and/or heading rate of change by an appropriate use of the vehicle control surfaces (Healey et al 1990). Unlike open sea operations, for vehicle missions in coastal areas and confined waters, the way point sequence must be very dense so that satisfactory path accuracy is maintained. One efficient way of maneuvering through a given way point sequence is by using a line-of-sight guidance law which commands a heading angle that is directly related to the line-of-sight angle between the vehicle position and a desired destination point. The vehicle controller is then an orientation control law which delivers the commanded heading. Previous studies (Papoulias 1991, 1992), have demonstrated that this scheme is guaranteed stable only if the way point separation is above some critical value. This conclusion is true regardless of the particular form of the line-of-sight guidance or the heading control law used. Similar results hold for vertical plane guidance (Papoulias 1992), although additional instabilities are possible here due to the existence of the metacentric height. In this work we analyze the turning rate guidance and control problem in the horizontal plane, where the guidance law demands a specific yaw rate response from the controller. A linear state feedback with a feedforward term (Friedland 1986) control law is used, while two different guidance schemes are considered. The first, a cross track error guidance, is very popular in land-based robotic applications

(Kanayama et al 1990), and the second, a proportional guidance law, is predominantly used in aerospace applications and interception/evasion problems (Brainin & McGhee 1968). Stability analysis is performed and bifurcation theory techniques (Hassard & Wan 1978, Guckenheimer & Holmes 1983) are utilized in order to assess the dynamics of the system upon initial loss of stability. All computations are performed for the Naval Postgraduate School autonomous test-bed vehicle for which a complete set of geometric properties and hydrodynamic characteristics is available (Bahrke 1992). Unless otherwise mentioned, all results are presented in standard dimensionless form with respect to the vehicle length $\ell = 2.3$ m and nominal forward speed $u = 0.6$ m/s, which corresponds to a Froude number of 0.13. At these conditions, the vehicle is very maneuverable due to a total of four rudder surfaces with a maximum turning rate of about 9 deg per second and a turning radius of less than two vehicle lengths.

1. Problem formulation

In this section we present the vehicle equations of motion in the horizontal plane. The control law is based on the dynamic equations in sway and yaw, whereas guidance is achieved through the use of the kinematic relations.

Equations of motion

Restricting our attention to the horizontal plane, the mathematical model consists of the nonlinear sway and yaw equations of motion. In a moving coordinate frame fixed at the vehicle's geometrical center (see Fig. 1), the maneuvering equations of motion are

$$m(\dot{v} + ur + x_G \dot{r}) = Y_r \dot{r} + Y_v \dot{v} + Y_r ur + Y_v uv + Y_\delta u^2 \delta - 0.5\rho C_D f h(\xi)(v + \xi r)|v + \xi r| d\xi \quad (1)$$

$$I_z \dot{r} + mx_G(\dot{v} + ur) = N_r \dot{r} + N_v \dot{v} + N_r ur + N_v uv + N_\delta u^2 \delta - 0.5\rho C_D f h(\xi)(v + \xi r)|v + \xi r| d\xi \quad (2)$$

where u is the vehicle forward speed, v and r are the relative sway and yaw velocities of the moving vehicle with respect to the water, and the rest of the symbols are explained in the Nomenclature. Equations (1) and (2) can be written as two first-order decoupled equations in the form

$$\dot{v} = a_{11}uv + a_{12}ur + b_1 u^2 \delta + d_v(v, r) \quad (3)$$

$$\dot{r} = a_{21}uv + a_{22}ur + b_2 u^2 \delta + d_r(v, r) \quad (4)$$

*Assistant professor, Department of Mechanical Engineering, Naval Postgraduate School, Monterey, California.

Manuscript received at SNAME headquarters September 23, 1992; revised manuscript received February 24, 1993.

y

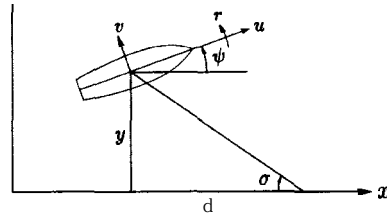


Fig. 1 Vehicle geometry and definitions of symbols

$$\dot{v} = a_{11}uv + a_{12}ur + b_1u^2\delta \quad (5)$$

$$\dot{r} = a_{21}uU + a_{22}ur + b_2u^2\delta \quad (6)$$

has the form

$$\delta = k_v v + k_r r \quad (7)$$

where k_v, k_r are the feedback gains. By substituting (7) into (5) and (6) we can find the closed loop characteristic equation

$$\lambda^2 + A_1\lambda + A_2 = 0 \quad (8)$$

where

$$A_1 = -[a_{11} + a_{22} + (b_1k_v + b_2k_r)u]u, \text{ and}$$

$$A_2 = [a_{11}a_{22} - a_{12}a_{21} + (b_1a_{22} - b_2a_{12})uk_v + (b_2a_{11} - b_1a_{21})uk_r]u^2.$$

If the desired characteristic equation is

$$\lambda^2 + \alpha_1\lambda + \alpha_2 = 0 \quad (9)$$

we can equate the coefficients of (8) and (9) and get the following system of linear equations

$$\begin{aligned} k_v b_1 u^2 + k_r b_2 u^2 &= -\alpha_1 - (a_{11} + a_{22})u \\ k_v (a_{22}b_1 - a_{12}b_2)u^3 + k_r (a_{11}b_2 - a_{21}b_1)u^3 \\ &= \alpha_2 - (a_{11}a_{22} - a_{12}a_{21})u^2 \end{aligned}$$

to be solved for the gains k_v and k_r .

The coefficients α_1, α_2 of the desired characteristic equation (9) can be specified according to standard second-order system transient response specifications (Friedland 19921. In

where the coefficients a_{ij}, b_i are functions of the hydrodynamic derivatives, geometric properties, and rudder coefficients. The terms $d_v(v, r)$ and $d_r(v, r)$ represent the contributions from the quadratic drag terms in (1) and (2). In the above form, the equations of motion are valid for both small and large drift angles. Drag related terms are relatively small for regular cruising operations, $u \gg (v + xr)$, and the vehicle response is, therefore, predominantly linear. For a vehicle operating near hover, $u \ll (v + xr)$, the quadratic drag forces dominate the response. The surge velocity u is clearly affected during the turn due to the added drag in turning. For the purposes of this study it is assumed to be constant. This is a valid approximation since experimental experience has shown that the propulsion control law is, in general, capable of keeping the forward speed relatively constant at the commanded value (Bahrke 19921.

Feedback control

A linear rudder feedback control law based on the linearized set of equations (3) and (4),

Nomenclature

a = open loop state coefficients in v, r model
 A = linearized system matrix
 b_i = open loop rudder coefficients in v, r model
 C_D = drag coefficient
 d = proportional guidance law preview distance
 I = vehicle mass moment of inertia
 \mathcal{H} = cubic stability coefficient
 k_v, k_r = control law feedback gains
 k_c or k_0 = control law feedforward gain
 $k\psi, k_r$ = cross track error guidance gains
 $k_v, k\sigma$ = proportional guidance gains
 m = vehicle mass
 N = yaw moment
 N_a = derivative of N with respect to a
 PAH = Poincare-Andronov-Hopf bifurcation
 r = yaw rate
 r_c = commanded yaw rate
 R = polar coordinate of transformed reduced system
 t = time

T = matrix of eigenvectors of A
 T_0 = zeroth-order approximation of limit cycle period
 T_C = control law time constant
 T_G = guidance law time constant
 u = vehicle forward speed
 v = sway velocity
 v_0 = ratio of steady-state sway velocity to steady-state turning rate
 \mathbf{x} = state variables vector
 x_G = body-fixed coordinate of vehicle center of gravity
 y = deviation off commanded path
 Y = sway force
 Y_a = derivative of Y with respect to a
 \mathbf{z} = state variables vector in canonical form
 z_1, z_2 = critical variables of \mathbf{z}
 z_3, z_4 = stable coordinates of \mathbf{z}

Greek symbols

α_i = coefficients of desired control characteristic equation

α' = derivative of α with respect to d evaluated at d_{crit}
 β_i = coefficients of desired guidance characteristic equation
 δ = rudder angle
 δ_{sat} = saturation level of rudder angle
 ϵ = difference between a bifurcation parameter and its critical value
 θ = polar coordinate of transformed reduced system
 ψ = vehicle heading angle
 σ = line-of-sight angle
 ω_c = positive imaginary part of critical pair of eigenvalues evaluated at critical point
 ω' = derivative of ω with respect to bifurcation parameter evaluated at critical value

this work we use the controller time constant, T_c , as the parameter. Then the desired characteristic equation is

$$\left(\lambda + \frac{1}{T_c}\right)^2 = 0 \quad \text{or} \quad \lambda^2 + \frac{2}{T_c}\lambda + \frac{1}{T_c^2} = 0$$

and comparing with (9) we see that

$$\alpha_1 = \frac{2}{T_c}, \quad \alpha_2 = \frac{1}{T_c^2} \quad (10)$$

Specification of a controller time constant T_c then determines the feedback gains k_v, k_r uniquely.

Feedforward control

The control law (7) guarantees stability of $v = r = 0$ of (5) and (6), in other words, straight line motion at an arbitrary heading. When the commanded angular velocity r_c is non-zero the control law is slightly modified to

$$\delta = k_v u + k_r (r - r_c) + k_c r_c \quad (11)$$

where k_c is the feedforward gain. The feedback gains k_v, k_r remain the same since the drag terms $d_v(v, r), d_r(v, r)$ are small and, therefore, the linearized dynamics of (3) and (4) around r_c do not differ significantly from (5) and (6). The feedforward gain k_c is computed based on steady-state accuracy requirements. At steady state, equations (5) and (6) yield

$$v = \frac{b_1 a_{22} - b_2 a_{12}}{b_2 a_{11} - b_1 a_{21}} r_c, \quad \delta = \frac{a_{21} a_{12} - a_{11} a_{22}}{(b_2 a_{11} - b_1 a_{21}) u} \quad (12)$$

Substituting (12) into (11) and requiring that $r = r_c$ at steady state we can solve for k_c and finally write the control law (11) in the form

$$\delta = k_v u + k_r r - k_0 \alpha_2 r_c \quad (13)$$

where

$$k_0 = \frac{1}{(b_2 a_{11} - b_1 a_{21}) u^3} \quad (14)$$

With the above feedforward gain the control law is complete. It should be mentioned that all gains k_v, k_r, k_0 depend explicitly on the forward speed u and are, therefore, continuously updated every time a different forward speed is commanded.

The feedforward gain k_0 computed from (14) ensures that the steady-state turning rate r equals the commanded value r_c for the linear system (5) and (6). In general, we can see from (3) and (4) that at steady state $r \neq r_c$ unless $d_v = d_r = 0$. As the controller time constant T_c is decreased, the control law becomes tighter and the steady-state error $|r - r_c|$ will be smaller. In practice, the above steady-state error could not be made zero due to uncertainties in the vehicle hydrodynamic description and other unmodeled dynamics. One way to ensure steady-state accuracy in r would be to abandon the use of the feedforward gain k_0 and to introduce integral control. This approach is not favored since it results, in general, in oscillatory transient response (Friedland 1992). The other alternative is to use a time varying r_c such that convergence to a specified geographical path is achieved. This is accomplished through the introduction of the guidance law presented in the following sections.

Cross track error guidance

In order to achieve path control to a commanded route in the horizontal plane, the commanded turning rate r_c must be appropriately selected. This constitutes the guidance law

design. Without loss in generality we can assume that the commanded path is a straight line. This is not a very restrictive assumption since every smooth path can be discretized into a series of straight-line segments as accurately as desired.

The guidance law is based solely on kinematics, whereas vehicle dynamics are handled by the rudder control law. Guidance law development is therefore based on

$$\dot{\psi} = r_c \quad (15)$$

$$\dot{y} = u \sin \psi \quad (16)$$

where r_c is the commanded turning rate and the lateral velocity v is assumed to be zero in (16). Cross track error guidance is achieved by

$$r_c = k_\psi \psi + k_y y \quad (17)$$

The closed loop characteristic equation of (15), (16), and (17) is

$$\lambda^2 - k_\psi \lambda - k_y u = 0 \quad (18)$$

If the desired characteristic equation is

$$\lambda^2 + \beta_1 \lambda + \beta_2 = 0 \quad (19)$$

the guidance law gains k_ψ, k_y are obtained by equating the coefficients of (18) and (19)

$$k_\psi = -\beta_1, \quad k_y = -\frac{\beta_2}{u} \quad (20)$$

Analogously to the control law design, if the time constant of the guidance law is selected to be T_G , then (20) results in

$$k_\psi = -\frac{2}{T_G}, \quad k_y = -\frac{1}{T_G^2 u} \quad (21)$$

Selection of T_G then determines k_ψ and k_y uniquely.

Although this development followed the small angle approximation $\sin \psi \approx \psi$, it is not difficult to see that negative values of k_ψ and k_y guarantee stability of the nonlinear system (15) and (16). The associated total energy of the system is

$$E(\psi, y) = \frac{1}{2} \dot{\psi}^2 - k_y u (1 - \cos \psi)$$

which can be viewed as the sum of kinetic and potential energy. Using (15) and (17) this is written as

$$E(\psi, y) = \frac{1}{2} (k_\psi \psi + k_y y)^2 - k_y u (1 - \cos \psi)$$

We note that $E(\psi, y)$ provides a Lyapunov function candidate for (15) and (16) since $E(0, 0) = 0$ at the unique equilibrium $(\psi, y) = (0, 0)$ and $E(\psi, y) > 0$ for $(\psi, y) \neq (0, 0)$, because $k_y < 0$. Moreover, we have

$$\begin{aligned} \dot{E} &= \frac{\partial E}{\partial \psi} \cdot \frac{d\psi}{dt} + \frac{\partial E}{\partial y} \cdot \frac{dy}{dt} \\ &= [(k_\psi \psi + k_y y) k_\psi - k_y u \sin \psi] (k_\psi \psi + k_y y) \\ &\quad + (k_\psi \psi + k_y y) k_y u \sin \psi \\ &= k_\psi (k_\psi \psi + k_y y)^2 \end{aligned}$$

which, since $k_\psi < 0$, is negative semi-definite. Therefore, Lyapunov's theorem guarantees stability of the nonlinear system (15) and (16) (Guckenheimer & Holmes 1983).

Proportional guidance

Proportional guidance with an integral term (Brainin & McGhee 1968) is achieved by

$$r_c = k_\sigma \dot{\sigma} + k_\sigma (\sigma - \psi) \quad (22)$$

In this fashion, the commanded turning rate attempts to close in on the difference between the vehicle heading ψ and the line-of-sight angle σ . The additional term which is proportional to the line-of-sight rate of change $\dot{\sigma}$ adds damping in cases where σ changes rapidly in time such as obstacle-avoidance, object-recognition, or terrain-following tasks. The line-of-sight angle is defined as the angle between the vehicle longitudinal axis and a target point located ahead of the vehicle on the nominal path at a constant preview distance d , as shown in Fig. 1. For the straight-line nominal path case we have

$$\sigma = -\tan^{-1} \frac{y}{d} \quad (23)$$

The proportional guidance characteristic equation is obtained from (15), (16), (22), and (23) as

$$\lambda^2 + \left(\frac{uk_r}{d} + k_\sigma \right) \lambda + \frac{k_\sigma u}{d} = 0 \quad (24)$$

and by comparing coefficients of (19) and (24) we get

$$k_r = \frac{\beta_2 d}{u}, \quad k_\sigma = \frac{\beta_1 du - \beta_2 d^2}{u^2} \quad (25)$$

where β_1, β_2 are explicit functions of the guidance law time constant T_G , as before.

2. Stability conditions

The turning rate control law developed in the foregoing section was designed to guarantee convergence to a constant commanded value of r_c , as well as to a series of step changes in r_c . The controller time constant T_C is inversely related to the bandwidth of the closed-loop (v, r) system (Friedland 1986) and this means that progressively smaller T_C values will ensure following of a time-varying commanded value $r_c(t)$ with smaller steady-state error. The common characteristic of both cross track error and proportional guidance laws, however, is that the commanded value r_c is a function of the vehicle state. This generates an additional loop encompassing the closed-loop steering dynamics and unless proper conditions are met, this outer loop may have a destabilizing effect. The purpose of this section is to establish these conditions explicitly so that stability of the combined guidance and control scheme is guaranteed. In particular, we seek those (T_C, T_G) combinations that result in motion stability. From the design point of view this is needed for the following reason: Smaller values of (T_C, T_G) result in a very responsive guidance and control law with excellent path-keeping capabilities. On the other hand, there is a limit on the values of (T_C, T_G) based on sensor noise. Therefore, in practice one should select the smallest possible (T_C, T_G) combination that guarantees stability as established through the analysis of this sections and Section 3.

Cross track error guidance

The complete system is given by the vehicle dynamic and kinematic equations

$$\dot{\psi} = r \quad (26)$$

$$\dot{v} = a_{11}uv + a_{12}ur + b_1u^2\delta \quad (27)$$

$$\dot{r} = a_{21}uv + a_{22}ur + b_2u^2\delta \quad (28)$$

$$\dot{y} = u \sin \psi + v \cos \psi \quad (29)$$

and the combined guidance and control law

$$\begin{aligned} \delta &= k_v v + k_r r - k_0 \alpha_2 r_c \\ &= k_v v + k_r r - k_0 \alpha_2 (k_\psi \psi + k_y y) \end{aligned} \quad (30)$$

In a compact vector notation the linearized form of the system is written as

$$\dot{\mathbf{x}} = \mathbf{A}\mathbf{x}, \quad \mathbf{x} = [\psi, v, r, y]^T \quad (31)$$

where the linearization is performed around the nominal equilibrium state $\psi = v = r = y = 0$. Motion stability is then established by the eigenvalues of \mathbf{A} : if all have negative real parts the nominal straight-line motion is dynamically stable, while if at least one eigenvalue of \mathbf{A} is positive, stability is lost. Writing out the characteristic equation of (31) we get

$$\lambda^4 + B\lambda^3 + C\lambda^2 + D\lambda + E = 0 \quad (32)$$

where

$$B = \alpha_1$$

$$C = \alpha_2 - (b_1\beta_2 + b_2u\beta_1)uk_0\alpha_2$$

$$D = \alpha_2\beta_1 + d_1\alpha_2\beta_2$$

$$E = \alpha_2\beta_2$$

and

$$d_1 = \frac{b_2 + b_2a_{12} - b_1a_{22}}{(b_2a_{11} - b_1a_{21})u}$$

If we apply Routh's criterion to the quartic (32) we find the following two active conditions for stability

$$BCD - B^2E - D^2 > 0, \quad \text{and} \quad (33)$$

$$D > 0 \quad (34)$$

Explicit evaluation of conditions (33) and (34) results in

$$T_C < \frac{2[T_G^2 - (b_1 + 2b_2T_Gu)uk_0](2T_G + d_1)}{4T_G^2 + (2T_G + d_1)^2} \quad (35)$$

$$T_G > \frac{1}{2} d_1 \quad (36)$$

In our problem, condition (36) is always satisfied, and, therefore, the only active stability condition is (35) which demands that for a given guidance time constant T_G , the controller time constant T_C must be less than a computable critical threshold. Since smaller values of T_C correspond to a tighter control law, this result is physically realizable in the sense that the control law must be sufficiently more responsive than the guidance law to guarantee path stability.

A plot of our stability condition (35) is presented in Fig. 2, where all variables are given in dimensionless form with respect to the vehicle length and forward speed. For large values of T_G the asymptotic form of (35) is $T_C < 0.5T_G + \text{const.}$, or any increase in the guidance law responsiveness must be accompanied by double the increase in the autopilot responsiveness.

If condition (35) is not satisfied, one pair of complex conjugate roots of (32) possesses positive real parts and as a result the response of the vehicle is oscillatory. The zeroth-

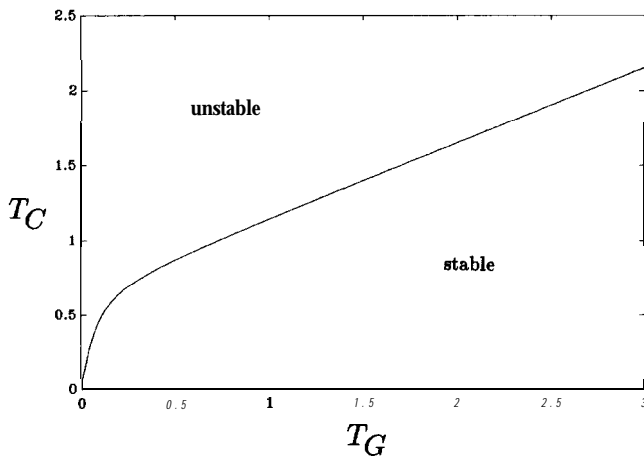


Fig. 2 Cross track error guidance: critical value of T_C versus T_G

order approximation for the period of the oscillatory response is

$$T_0 = \frac{2\pi}{\omega_0} \quad (37)$$

where ω_0 is the absolute value of the imaginary part of the critical pair of eigenvalues. The above stability analysis results are confirmed by the time simulation of Fig. 3, for $T_G = 0.5$ and two different values of T_C . For this value of T_G the critical value of T_C is 0.87 and equation (37) predicts a period of 3.6 dimensionless seconds, which is close to the numerical integration results observed in the figure. As T_C is decreased below its critical value, stability of straight-line motion is guaranteed. The time simulations of Fig. 4 present a slightly different picture, however. Here $T_G = 0.25$ and the critical $T_C = 0.6925$. For $T_C = 0.7$ a large-amplitude periodic motion is developing, unlike the case of Fig. 3 where the periodic solution is concentrated in the vicinity of the nominal equilibrium. The period of this periodic solution is significantly larger than the value of $T_0 = 2$ predicted by (37). Furthermore, for $T_C = 0.4 < 0.6925$ it appears that convergence to the nominal equilibrium is guaranteed only for initial conditions that are located very close to equilibrium. The

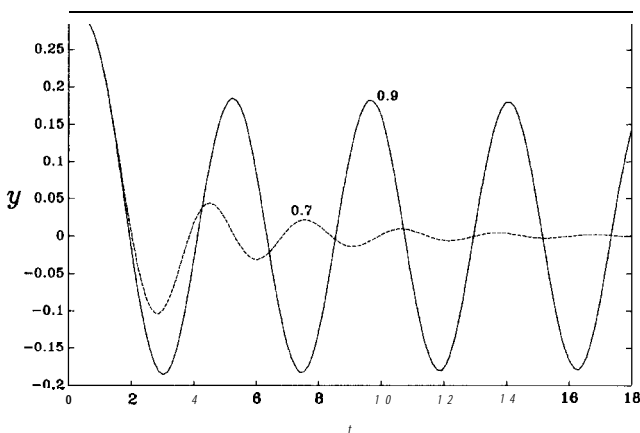


Fig. 3 Cross track error guidance: simulation results for $T_G = 0.5$ and two different values of T_C

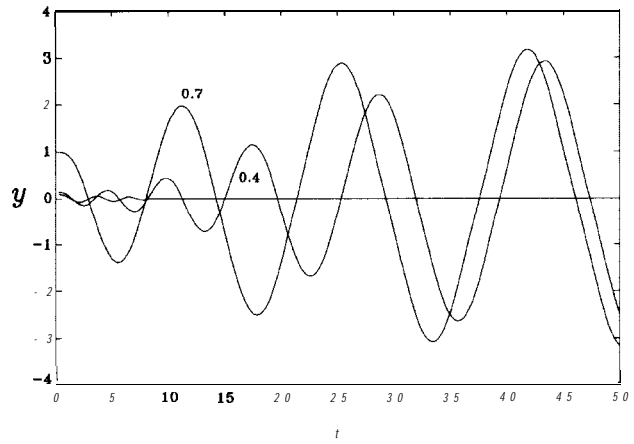


Fig. 4 Cross track error guidance: simulation results for $T_G = 0.25$ and two different values of T_C

above difference in the response between the two cases, $T_G = 0.5$ and $T_G = 0.25$, cannot be predicted by our stability analysis so far, and is the subject of studies performed in Section 3.

Significance of feedforward control

At steady state, equations (26-29) yield $\psi = v = r = \delta = 0$, and equation (30) $y = 0$. This is true regardless of any hydrodynamic modeling inaccuracies or the value of the feedforward term k_0 in the control law. It appears then that the guidance law ensures steady-state accuracy without the need for the feedforward term k_c in the control law (11). Although this is a valid statement as far as steady-state accuracy is concerned, its effect on the stability of the combined guidance and control scheme needs to be investigated. To do this we set $k_c = 0$ in (11) and we form the new linearized system matrix as in (31). The characteristic equation takes the form of (32) with

$$\mathbf{B} = \alpha_1$$

$$\mathbf{c} = \alpha_2 - (b_1 + b_2)u^2 k_r \beta_1$$

$$D = -(b_2 + b_2 a_{12} - b_1 a_{22})u^2 k_r \beta_2 + (b_2 a_{11} - b_1 a_{21})u^3 k_r \beta_1$$

$$E = (b_2 a_{11} - b_1 a_{21})u^3 k_r \beta_2$$

The two stability conditions are (33) and (34). Condition (33) results in a (T_G, T_C) locus, similar as before. Condition (34) is violated when k_r crosses zero, which determines a critical value of T_C given as the solution to

$$C_2 T_C^2 + C_1 T_C + C_0 = 0 \quad (38)$$

where

$$C_2 = (a_{11} + a_{22})(a_{21} b_1 - a_{12} b_2)u^2 - (a_{11} a_{22} - a_{12} a_{21})b_1 u^2,$$

$$C_1 = 2(a_{22} b_1 - a_{12} b_2)u, \text{ and}$$

$$C_0 = b_1.$$

Results are presented in Fig. 5, where three distinct regions of stability are clear. Region I is the region of stability and in Region II one pair of complex conjugate roots of (32) has positive real parts with oscillatory vehicle response as seen earlier. In Region III where T_C is greater than the constant critical value determined by (38), one real root of (32) is positive. In the latter case, the dynamic response of the system is associated with more complicated bifurcation phenomena,

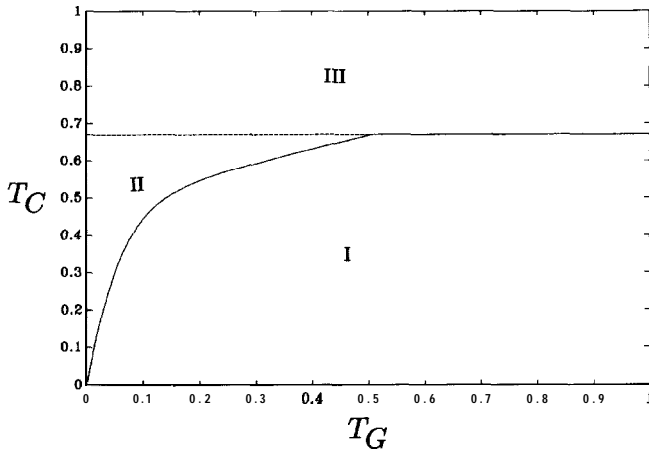


Fig. 5 Cross track error guidance: critical value of T_C versus T_G in absence of feedforward control

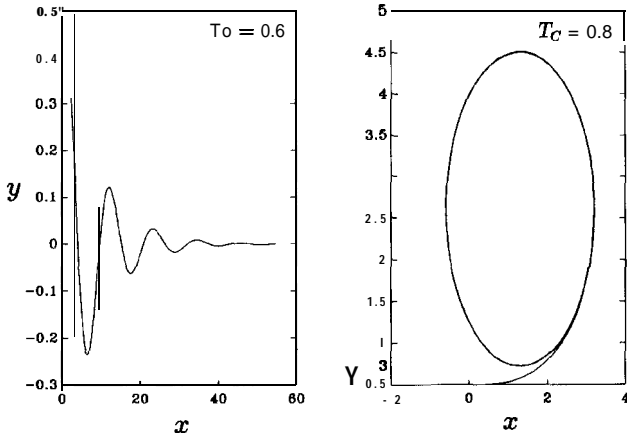


Fig. 6 Cross track error guidance: simulation results for $T_G = 0.8$ and two different values of T_C in absence of feedforward control

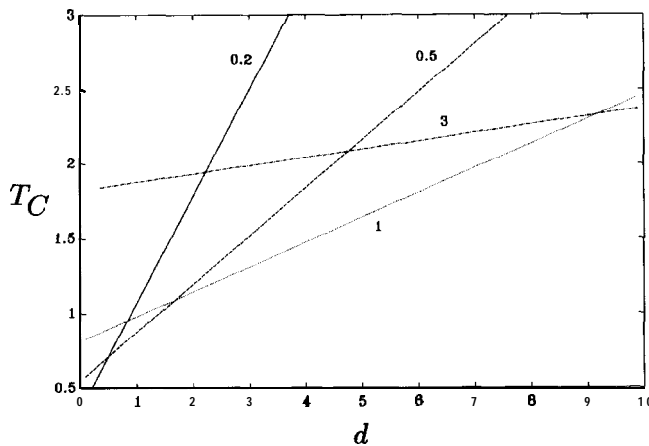


Fig. 7 Proportional guidance: critical value of T_C versus d for different values of T_G

as demonstrated by the numerical simulations of Fig. 6 for which $T_G = 0.8$. When $T_C = 0.6$, the parameter range is within Region I and the path deviation converges to zero as expected. When $T_C = 0.8$, the parameter range is within Region III and a pathological convergence to a limit cycle in the (x, y) plane is observed associated with constant values of the sway velocity v and turning rate r , and linearly increasing (modulo 2π) heading angle ψ . These phenomena are of limited practical significance since they can be easily avoided by the introduction of k_c and can be further analyzed, if desired, by using techniques similar to the vertical plane steady-state bifurcations case considered in Papoulias (1992). Nevertheless, the results demonstrate the importance on motion stability that the feedforward term k_c carries in the control law (11) despite the fact that feedforward control normally affects only steady-state accuracy.

Proportional guidance

Stability analysis for the proportional guidance scheme proceeds in a similar fashion. The linearized guidance and control law is obtained from (22) and is analogous to (30)

$$\delta = k_1\psi + k_2v + k_3r + k_4y \quad (39)$$

where

$$k_1 = k_0\alpha_2 \left(k_\sigma + \frac{u}{d} k_\delta \right)$$

$$k_2 = k_v + \frac{k_\delta}{d} k_0\alpha_2$$

$$k_3 = k_r$$

$$k_4 = \frac{k_\sigma}{d} k_0\alpha_2$$

Substitution of (39) in (27) and (28) produces a linear system in the form of (31). The characteristic equation of (31) is written in the same form as (32) where the coefficients are given by

$$B = -(a_{11} + a_{22})u - b_1u^2k_2 - b_2u^2k_3$$

$$C = (b_1a_{22} - b_2a_{12})u^3k_2 + (b_2a_{11} - b_1a_{21})u^3k_3 + (a_{11}a_{22} - a_{12}a_{21})u^2 - b_2u^2k_1 - b_1u^2k_4$$

$$D = (b_2a_{11} - b_1a_{21})u^3k_1 + (b_1a_{22} - b_2a_{12} - b_2)u^3k_4$$

$$E = (b_2a_{11} - b_1a_{21})u^4k_4$$

The stability conditions are the same as (33) and (34). For a given (T_C, T_G) combination, there exists a critical value of d for stability. This is computed from (33) as the solution to

$$B_2(C_2D_1 - B_2E_1)d^2 + [D_1(B_1C_2 + B_2C_1) - 2B_1B_2E_1]d + (B_1C_1D_1 - B_1^2E_1 - D_1^2) = 0 \quad (40)$$

where

$$B_1 = \alpha_1 - b_1k_0\alpha_2\beta_1u$$

$$B_2 = b_1k_0\alpha_2\beta_2$$

$$C_1 = \alpha_2 + (b_1a_{22} - b_2a_{12})u^2k_0\alpha_2\beta_1 - b_1uk_0\alpha_2\beta_2 - b_2u^2k_0\alpha_2\beta_1$$

$$C_2 = -(b_1a_{22} - b_2a_{12})uk_0\alpha_2\beta_2$$

$$D_1 = (b_2a_{11} - b_1a_{21})u^3k_0\alpha_2\beta_1 + (b_1a_{22} - b_2a_{12} - b_2)u^2k_0\alpha_2\beta_2$$

$$E_1 = (b_2a_{11} - b_1a_{21})u^3k_0\alpha_2\beta_2$$

Assuming that $D_1 > 0$ is satisfied, equation (40) determines

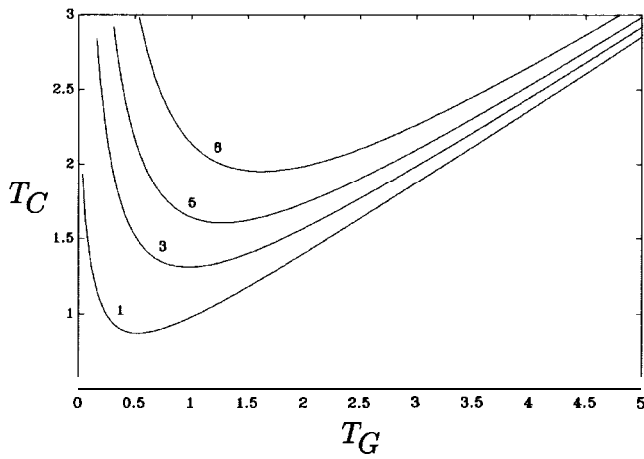


Fig. 8 Proportional guidance: critical value of T_C versus T_G for different values of d

the least required preview distance d for stability. Typical results in the (d, T_C) parameter plane are shown in Fig. 7 for different values of the guidance time constant T_G . Stability is guaranteed for values of T_C below the critical curve. It can be seen that for increasing values of T_G , proportional guidance is stable regardless of the value of d provided that T_C is sufficiently small. For decreasing values of T_G , stability is guaranteed only for values of d larger than some critical value so that the guidance dynamics are sufficiently slowed down.

For a given (T_G, d) combination, there exists a critical value of T_C for stability. This is computed from (33) as the solution to

$$(4E' + D'^2)T_C^2 + 2(2B'E' - C'D')T_C + B'(B'E' - C'D') = 0 \quad (41)$$

where

$$B' = b_1 k_0 (\beta_2 d - \beta_1 u)$$

$$C' = 1 + (b_1 a_{22} - b_2 a_{12}) u k_0 (\beta_1 u - \beta_2 d) - b_1 u k_0 \beta_2 - b_2 u^2 k_0 \beta_1$$

$$D' = (b_2 a_{11} - b_1 a_{21}) u^3 k_0 \beta_1 + (b_1 a_{22} - b_2 a_{12} - b_2) u^2 k_0 \beta_2$$

$$E' = (b_2 a_{11} - b_1 a_{21}) u^3 k_0 \beta_2$$

Assuming that $D' > 0$ is satisfied, equation (41) determines the maximum allowable value of the controller time constant T_C for stability. Typical results in the (T_G, T_C) parameter plane are shown in Fig. 8 for different values of the preview distance d . Stability is guaranteed for values of T_C below the critical curve. It can be seen that, in general, the region of stability is enlarged for increasing values of T_G , which corresponds to a softer guidance law. The same conclusion holds for increasing values of the preview distance d . Figure 8 demonstrates the advantages that proportional guidance offers over cross track error guidance. Since two parameters affect stability, d and T_G , for each value of one we can select the other so that stability is maintained. As the value of d approaches zero, the (T_G, T_C) stability curve resembles in shape the critical curve for cross track error guidance. This means that, in a certain sense, cross track error guidance can be thought of as a limiting case of proportional guidance for very small values of the preview distance. Analytically, this can be shown as follows. Substituting (23) into (22) we can get the commanded turning rate r_c

for proportional guidance as a function of the inertial position y , its rate of change \dot{y} , and heading angle ψ

$$r_c = -k_\sigma \frac{d}{y^2 + d^2} \dot{y} - k_\sigma \left(\tan^{-1} \frac{y}{d} + \psi \right)$$

As $d \rightarrow 0$, we have that $y/d \ll 1$, since $y \ll d$ assuming straight line stability as $t \rightarrow \infty$. By expanding in Taylor series and keeping the first-order term only we get

$$r_c = -k_\sigma \frac{1}{d} \dot{y} - k_\sigma \left(\frac{y}{d} + \psi \right)$$

and substituting k_σ, k_σ from (25),

$$r_c = -\frac{\beta_1 u - \beta_2 d}{u^2} \dot{y} - \frac{\beta_2}{u} y - \frac{\beta_2 d}{u} \psi$$

If we substitute the linearized expression for the inertial position rate $\dot{y} = u\psi$ —assuming $v = 0$ as in the case of cross track error guidance—we get

$$r_c = \beta_1 \psi - \frac{\beta_2}{u} y$$

which has the same form as (17) using the cross track error guidance gains (20).

3. Bifurcation analysis

In this section we apply bifurcation theory to the study of dynamic interactions between cross track error and proportional guidance and the turning rate control law. The purpose here is to assess the dynamic response of the vehicle upon initial loss of stability of straight-line motion and to explain the numerical simulation results observed in Figs. 3, 4, and 6.

Bifurcations to periodic solutions

The most common loss of stability case is where condition (33) is violated and (34) is satisfied. The corresponding parameter values give rise to Poincare-Andronov-Hopf (PAH) bifurcation points: at precisely these points one pair of complex conjugate eigenvalues of (31) possesses zero real parts. The most significant result of this PAH bifurcation is the generation of a family of periodic solutions with continuously increasing amplitude as the parameter value moves away from its critical value (Guckenheimer & Holmes 1983). These periodic solutions exist for parameter values where the nominal equilibrium is either stable or unstable, and they can be orbitally stable or unstable.

In order to establish direction of PAH bifurcations, and limit cycle stability, we have to isolate the main nonlinear terms in the equations of motion (26-29). Due to port/starboard symmetry, when these equations are expanded in Taylor series, second-order terms vanish identically and the first remaining nonzero terms are third order. The rudder control effort δ appears from (13) to be linear, but in reality it saturates at $\pm \delta_{\text{sat}}$. Since this hard saturation function is non-analytic we substitute it by a hyperbolic tangent function of the form

$$\delta = \delta_{\text{sat}} \tanh \left(\frac{k_v u + k_r r - k_0 \alpha_2 r_c}{\delta_{\text{sat}}} \right) \quad (42)$$

where the saturation limit δ_{sat} is typically around 0.4 radians. It should be mentioned that any analytic function with limits $\pm \delta_{\text{sat}}$ and slope at the origin given by (13) can be used

in lieu of (42), the actual choice does not significantly affect the results that follow.

After performing the above third-order Taylor series expansion, we write the equations of motion (26–29) in the form

$$\dot{\mathbf{x}} = \mathbf{A}\mathbf{x} + \mathbf{g}(\mathbf{x}) \quad (43)$$

where \mathbf{A} is the linearized system matrix and $\mathbf{g}(\mathbf{x})$ contains the leading nonlinear terms. If \mathbf{T} is the matrix of eigenvectors of \mathbf{A} evaluated at the PAH bifurcation point, the transformation $\mathbf{x} = \mathbf{T}\mathbf{z}$ transforms system (43) into its normal coordinate form

$$\dot{\mathbf{z}} = \mathbf{T}^{-1}\mathbf{A}\mathbf{T}\mathbf{z} + \mathbf{T}^{-1}\mathbf{g}(\mathbf{T}\mathbf{z}) \quad (44)$$

Near the PAH bifurcation point:

$$\mathbf{T}^{-1}\mathbf{A}\mathbf{T} = \begin{bmatrix} \alpha'\epsilon & -(\omega_0 + \omega'\epsilon) & 0 & 0 \\ \omega_0 + \omega'\epsilon & \alpha'\epsilon & 0 & 0 \\ 0 & 0 & p & 0 \\ 0 & 0 & 0 & q \end{bmatrix}$$

where ϵ is the difference between the physical parameter value (such as T_C, T_G , or d) and its critical value, ω_0 is the absolute value of the imaginary part of the critical pair of eigenvalues at the bifurcation point, $\alpha'(\omega')$ is the derivative of the real (imaginary) part of the critical pair of eigenvalues evaluated at $\epsilon = 0$, and p, q are the remaining two negative eigenvalues of \mathbf{A} . In the new system of coordinates $\mathbf{z} = \mathbf{T}^{-1}\mathbf{x}$, the dynamics of (44) are governed by a reduced two-dimensional system z_1, z_2 , since the coordinates z_3, z_4 correspond to the eigenvalues p, q and are asymptotically stable. Since z_3, z_4 can be expressed in third order, at least, expressions in terms of z_1, z_2 (Guckenheimer & Holmes 1983), they do not affect our Taylor expansions in (44). Therefore, we can write the system in the critical coordinates z_1, z_2 in the form

$$\dot{z}_1 = \alpha'\epsilon z_1 - (\omega_0 + \omega'\epsilon)z_2 + r_{11}z_1^3 + r_{12}z_1^2z_2 + r_{13}z_1z_2^2 + r_{14}z_2^3 \quad (45)$$

$$\dot{z}_2 = (\omega_0 + \omega'\epsilon)z_1 + \alpha'\epsilon z_2 + r_{21}z_1^3 + r_{22}z_1^2z_2 + r_{23}z_1z_2^2 + r_{24}z_2^3 \quad (46)$$

where the coefficients r_{ij} are computable from the above Taylor expansions. If we introduce polar coordinates in the form

$$z_1 = \mathbf{R} \cos \theta, \quad z_2 = \mathbf{R} \sin \theta \quad (47)$$

and perform averaging over the cyclic coordinate θ from 0 to 2π , equations (45) and (46) result in the following reduced equation in the radial coordinate \mathbf{R} ,

$$\dot{\mathbf{R}} = \alpha'\epsilon \mathbf{R} + \mathcal{K} \mathbf{R}^3 \quad (48)$$

where

$$\mathcal{K} = \frac{1}{8} (3r_{11} + r_{13} + r_{22} + 3r_{24}) \quad (49)$$

From equation (48) we can see that:

1. If $\alpha' > 0$, then
 - (a) if $\mathcal{K} > 0$, then unstable period solutions coexist with the stable equilibrium for $\epsilon < 0$, and
 - (b) if $\mathcal{K} < 0$, then stable period solutions coexist with the unstable equilibrium for $\epsilon > 0$.
2. If $\alpha' < 0$, then
 - (a) if $\mathcal{K} > 0$, then unstable period solutions coexist with the stable equilibrium for $\epsilon > 0$, and

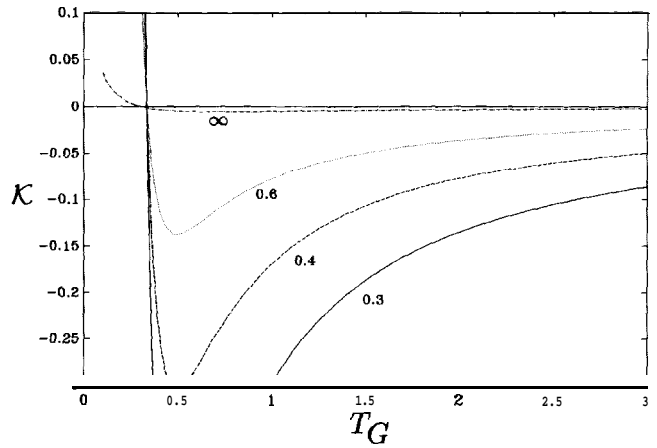


Fig. 9 Cross track error guidance: cubic coefficient \mathcal{K} versus T_G for different values of δ_{sat} .

(b) if $\mathcal{K} < 0$, then stable period solutions coexist with the unstable equilibrium for $\epsilon < 0$.

We refer to the $\mathcal{K} > 0$ cases as the subcritical, and the $\mathcal{K} < 0$ cases as the supercritical PAH bifurcations (Guckenheimer & Holmes 1983). In the following section we present results of this third-order analysis for both cross track error and proportional guidance schemes.

Results

A plot of the cubic coefficient \mathcal{K} versus T_G for the cross track error guidance case and for different values of the rudder saturation limit δ_{sat} is presented in Fig. 9. It can be seen that for $T_G < 0.334$, \mathcal{K} is positive and it becomes negative for larger T_G values. Therefore, for $T_G = 0.5$ which refers to the time simulations of Fig. 3, the corresponding PAH bifurcations are supercritical and a small-amplitude stable periodic solution surrounds the unstable nominal equilibrium as T_C becomes higher than its critical value (35). For $T_G = 0.25$, which refers to the time simulations of Fig. 4, the corresponding PAH bifurcations are subcritical since \mathcal{K} is positive. An unstable periodic solution coexists here with the stable nominal point for T_C less than its critical value. Convergence to the stable equilibrium point is ensured now only if the initial conditions fall within the unstable limit cycle, as Fig. 4 demonstrated. As is the case with many PAH bifurcations, the above unstable limit cycles change their stability and direction as the parameter T_G moves further away from the bifurcation point. Schematically, the above two cases are shown in Fig. 10. Solid lines correspond to stable and dotted lines to unstable nominal equilibrium, while solid curves correspond to stable and dotted curves to unstable periodic solutions. Both are viewed in increasing values of T_G and periodic solutions originate as T_G reaches its critical value for a given T_C . The progressive buildup of the amplitude of the periodic solutions for the supercritical case ver-

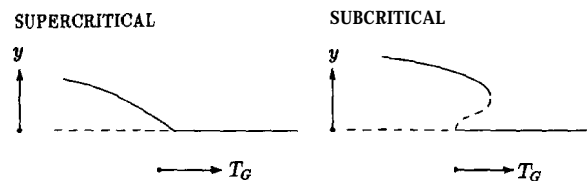


Fig. 10 Supercritical and subcritical PAH bifurcations

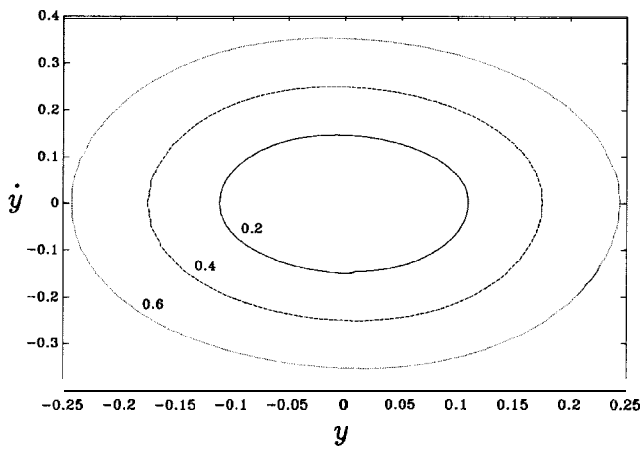


Fig. 11 Cross track error guidance: simulation results for $T_C = 0.9$, $T_G = 0.5$, and different values of δ_{sat}

sus the sudden amplitude enlargement for the subcritical case which was observed in Figs. 3 and 4 can be clearly seen,

The effect of the rudder saturation level which does not affect the linear stability analysis is also evident from Fig. 9. Although transitions between supercritical and subcritical bifurcations appear to be relatively insensitive to the value of δ_{sat} , the value of \mathcal{K} becomes less negative as δ_{sat} is increased. This means that rudder angle saturation has a stabilizing effect in this problem: upon initial loss of stability of straight-line motion, the stable limit cycle amplitudes are decreased for decreasing saturation values δ_{sat} . This result is in sharp contrast to orientation guidance laws where rudder angle saturation was found to induce a significant destabilizing effect (Papoulias 1991). This rudder saturation stabilizing effect is numerically demonstrated in Fig. 11, where limit cycles in the (y, \dot{y}) phase subspace are shown for $T_C = 0.9$ and $T_G = 0.5$, and for different rudder saturation levels δ_{sat} in radians.

Similar results in terms of the cubic coefficient \mathcal{K} for the proportional guidance case are presented in Figs. 12 and 13. Figure 12 shows \mathcal{K} versus T_C for different values of T_G for the PAH bifurcations of Fig. 7. For supercritical bifurcations

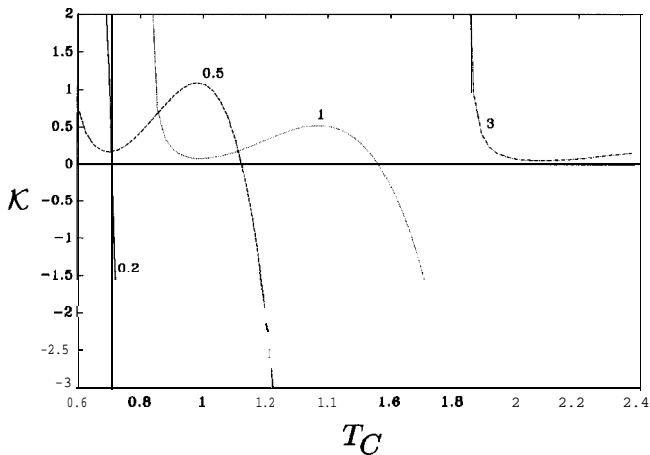


Fig. 12 Proportional guidance: cubic coefficient \mathcal{K} versus T_C for different values of T_G

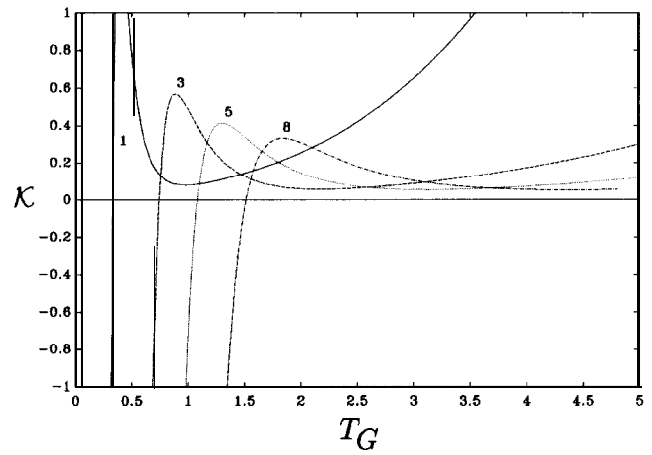


Fig. 13 Proportional guidance: cubic coefficient \mathcal{K} versus T_G for different values of d

to occur ($\mathcal{K} < 0$) it can be seen that the controller time constant T_C must be selected to be higher than a certain critical value. Figure 13 presents \mathcal{K} versus T_G for different values of d for the PAH bifurcation curves of Fig. 8. Supercritical bifurcations are ensured provided T_G is larger than a certain critical value which requires increasingly higher values of T_C as Fig. 12 suggested as well.

Side slip effects

The cross track error guidance law (17) was based on equations (15) and (16), which neglected the influence of side slip velocity v that exists as a result of the commanded turning rate τ_c . In order to analyze the potential benefits from incorporating side slip information on overall motion stability, we base the guidance law (17) on equation (15) and

$$\dot{y} = u \sin \psi + v_0 r_c \cos \psi \quad (50)$$

instead of (16), where

$$v_0 = \frac{b_1 a_{22} + a_{21}}{b_2 a_{11} - b_1 a_{21}}$$

and $v_0 r_c$ is the steady-state sway velocity that develops with the turning rate r_c . The closed-loop characteristic equation of (15), (50), and (17) is

$$\lambda^2 - (k_\psi + v_0 k_y) \lambda - k_y u = 0 \quad (51)$$

and by equating the coefficients of (19) and (51) we get the guidance gains

$$k_\psi = -\beta_1 + \frac{v_0 \beta_2}{u}, \quad k_y = -\frac{\beta_2}{u} \quad (52)$$

Typical results are shown in Fig. 14 in terms of the critical T_C versus T_G curve. It can be seen that introduction of appropriate side slip information results in an increase of the region of motion stability. This effect is more pronounced for small T_C values where the control law is more responsive and the amount of side slip is, therefore, larger. The increase in the region of stability is accompanied by an even more beneficial limit cycle stability as indicated by Fig. 15. It can be seen that the cubic coefficient \mathcal{K} is more negative when the side slip correction is active, which results in stronger supercritical PAH bifurcations with smaller limit cycle amplitudes after the initial loss of stability of straight-line motion.

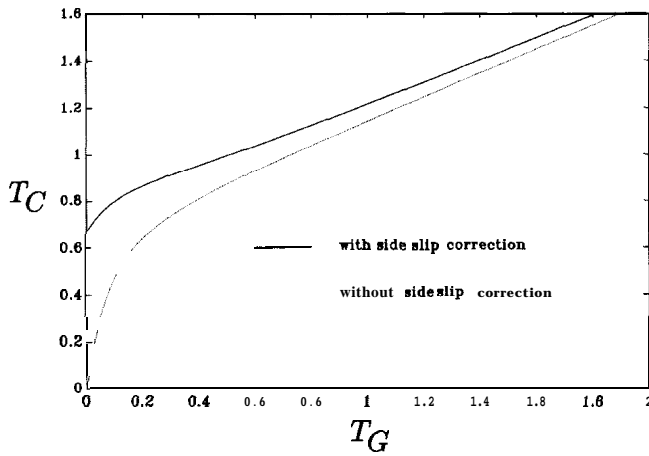


Fig. 14 Cross track error guidance: critical value of T_C versus T_G with and without side slip correction

Concluding remarks

Analysis of the dynamic response of a marine vehicle under coupled operation of turning rate guidance and control has been presented. Linear full-state feedback control has been employed for demonstration purposes with a feedforward term to ensure steady-state accuracy. Two turning rate guidance schemes were introduced and analyzed: cross track error and proportional guidance. Linear stability analysis was performed in order to evaluate regions of stability and instability of straight-line motion, and third-order nonlinear expansions were utilized in the analysis of Poincaré-Andronov-Hopf bifurcations. The primary conclusions of this study can be summarized as follows:

1. Loss of stability is possible if the control law is not sufficiently responsive compared to the dynamics of the guidance law. This is true for both cross track error and proportional guidance.
2. For better path-keeping characteristics it is required

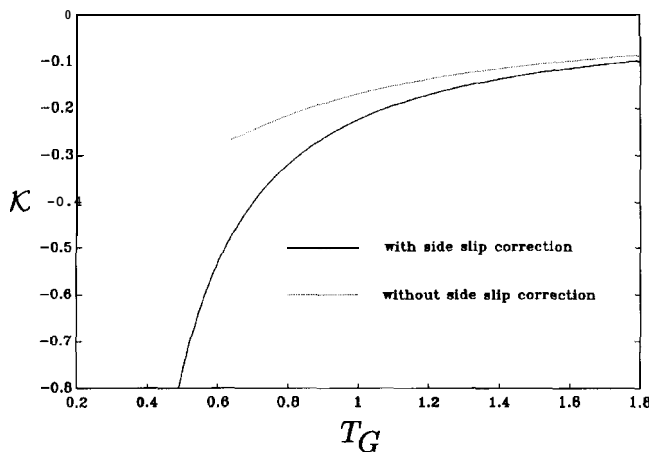


Fig. 15 Cross track error guidance: cubic coefficient K versus T_G with and without side slip correction

that the guidance law must be as responsive as possible. It was shown that, asymptotically, any increase in the guidance law responsiveness must be accompanied by double the increase in the autopilot responsiveness in order to maintain stability.

3. The feedforward term in the control law has significant effects on stability in spite of the fact that feedforward control usually affects only steady-state accuracy. It was shown that in the absence of the feedforward term additional instabilities are possible, and the domain of stability of straight-line motion is greatly reduced.

4. Proportional guidance was found to offer additional advantages on stability compared with cross track error guidance. It was shown that cross track error guidance can be obtained as the limiting case of proportional guidance as the preview distance approaches zero.

5. The main cases of loss of stability were identified as typical PAH bifurcations with the generation of periodic solutions. Third-order Taylor series expansion revealed the stability of the limit cycles. It was shown that stable limit cycles would exist for sufficiently slow control laws, while unstable limit cycles were created as a result of a very responsive control.

6. A nonlinear stabilizing effect of rudder saturation was established. This result, which does not affect the linear stability of the system, is unique to turning rate guidance; previous studies have revealed that rudder saturation results in a nonlinear destabilizing effect in the case of orientation guidance and control.

7. Finally, it was shown that appropriate side slip information in the design of the guidance law results in an appreciable enlargement of the region of stability of straight-line motion.

Acknowledgment

The author would like to recognize the financial support of the Naval Postgraduate School Direct Research Fund.

References

- BAHRKE, F. 1992 On-line identification of the speed, steering and diving response parameters of an autonomous underwater vehicle from experimental data. Mechanical engineer's thesis, Naval Postgraduate School, Monterey, Calif.
- BRAININ, S. M. AND MCGHEE, R. B. 1968 Optimal biased proportional navigation. *IEEE Transactions on Automatic Control*, 13, 4.
- FRIEDLAND, B. 1986 *Control System Design: An Introduction to State-Space Methods*, McGraw-Hill, New York.
- GUCKENHEIMER, J. AND HOLMES, P. 1983 *Nonlinear Oscillations, Dynamical Systems, and Bifurcations of Vector Fields*, Springer-Verlag, New York.
- HASSARD, B. AND WAN, Y. H. 1978 Bifurcation formulae derived from center manifold theory. *Journal of Mathematical Analysis and Applications*, 63, 297-312.
- HEALEY, A. J., MCGHEE, R. B., CRISTI, R., PAPOULIAS, F. A., KWAK, S. H., KANAYAMA, Y., AND LEE, Y. 1990 Mission planning, execution, and data analysis for the NPS AUV II autonomous underwater vehicle. Proceedings, NSF Workshop on Mobile Undersea Robotics, Monterey, Calif.
- KANAYAMA, Y., KIMURA, Y., NOGUCHI, T., AND MIYAZAKI, F. 1990 A stable tracking control method for an autonomous mobile robot. Proceedings, IEEE International Conference on Robotics and Automation, Cincinnati, Ohio.
- PAPOULIAS, F. A. 1991 Bifurcation analysis of line of sight vehicle guidance using sliding modes. *International Journal of Bifurcation and Chaos*, 1, 4.
- PAPOULIAS, F. A. 1992 Loss of stability of guidance and control laws for autonomous vehicles. *Dynamics and Stability of Systems*, 8, 1.
- PAPOULIAS, F. A. 1992 Dynamics and bifurcations of pursuit guidance for vehicle path keeping in the dive plane. *JOURNAL OF SHIP RESEARCH*, accepted for publication.